A Harmonic Balance Approach for Large-Scale Problems in Nonlinear Structural Dynamics

Allen R LaBryer, PhD Candidate
Peter J Attar, Assistant Professor
University of Oklahoma
Aerospace and Mechanical Engineering
2010 Oklahoma Supercomputing Symposium

Introduction

- Time-periodic phenomena are abundant in nature
- Can be analyzed experimentally or numerically
- Traditional approach to numerical simulation:
  - Capture the physics in language of mathematics
    - Partial differential equations (PDEs)
    - Natural oscillators tend to present themselves as nonlinear dynamical systems
  - Discretize the governing equations in space
    - Finite element method (FE) for structures
  - Temporal discretization
    - Time-marching methods (Newmark, HHTα)
    - Computationally expensive; transient effects
    - Efficient alternatives exist (harmonic balance)

Introduction

- Presented here: a novel time-domain solution method
  - High dimensional harmonic balance (HDHB) approach
  - Discuss its key features and limitations
  - Rapid computation of steady state solutions
  - Provide a framework for implementation into a nonlinear FE solver
- Demonstrate its capabilities
  - Solve three structural dynamics problems
  - Relevant to the field of flapping flight

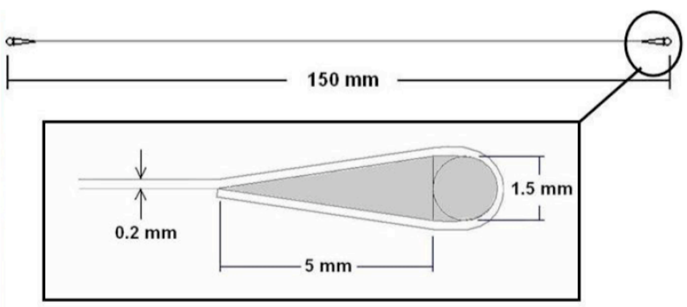

Plunging 1D string

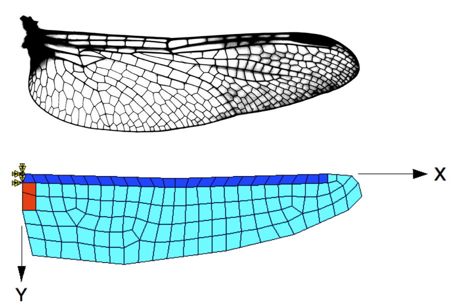

Flapping 2D dragonfly wing

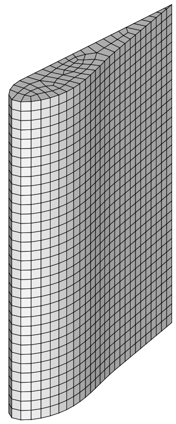

Oscillating 3D airfoil

Harmonic balance theory

- Begin with a general nonlinear dynamical system (FE eqns)

$$\mathbf{M}\ddot{\mathbf{X}} + \mathbf{C}\dot{\mathbf{X}} = \mathbf{F}(\mathbf{X},t)$$

- Assume the field variables are smooth and periodic in time
- Fourier series expansion of state vector and nonlinear restoring force vector

$$\mathbf{X}(t) = \hat{\mathbf{X}}^0 + \sum_{k=1}^{N_H}\left[\hat{\mathbf{X}}^{2k-1}\cos(k\omega t) + \hat{\mathbf{X}}^{2k}\sin(k\omega t)\right] \qquad \mathbf{F}(t) = \hat{\mathbf{F}}^0 + \sum_{k=1}^{N_H}\left[\hat{\mathbf{F}}^{2k-1}\cos(k\omega t) + \hat{\mathbf{F}}^{2k}\sin(k\omega t)\right]$$

- Classical harmonic balance (HB) method
  - Approach to solve for the Fourier coefficients $\mathbf{X}^k(t)$
  - Substitute Fourier expansions for $\mathbf{X}(t)$ and $\mathbf{F}(t)$ into the governing equation
  - Perform a Galerkin projection w.r.t. the Fourier modes to obtain

N_H = Chosen # of harmonics

$N_T = 2N_H + 1$

$$\omega^2\mathbf{A}^2\hat{\mathbf{Q}}\mathbf{M} + \omega\mathbf{A}\hat{\mathbf{Q}}\mathbf{C} - \hat{\mathbf{F}} = \mathbf{0} \qquad \hat{\mathbf{Q}} = \begin{bmatrix} \hat{x}_1^0 & \cdots & \hat{x}_{N_{dof}}^0 \\ \vdots & \hat{x}_i^k & \vdots \\ \hat{x}_1^{N_T} & \cdots & \hat{x}_{N_{dof}}^{N_T} \end{bmatrix}_{(N_T)\times(N_{dof})} \qquad \mathbf{A} = \begin{bmatrix} 0 & & & \\ & \mathbf{J}_1 & & \\ & & \ddots & \\ & & & \mathbf{J}_{N_H} \end{bmatrix}_{(N_T)\times(N_T)} \qquad \mathbf{J}_k = \begin{bmatrix} 0 & k \\ -k & 0 \end{bmatrix}$$

  - Using this procedure to solve large-scale nonlinear systems can be cumbersome
  - Overcome with the high dimensional harmonic balance (HDHB) approach

HDHB approach

- Introduction
- Numerical method
  - HDHB approach
  - Key features
  - FE implementation
- Application
  - Plunging 1D string
  - 2D dragonfly wing
  - Oscillating 3D airfoil
- Conclusions

- Problem is cast from Fourier domain into the time domain
- Fourier coefficients are related to time domain variables through a discrete Fourier transform operator **E**

$$\hat{\mathbf{Q}} = \mathbf{E}\tilde{\mathbf{Q}} \qquad \hat{\mathbf{F}} = \mathbf{E}\tilde{\mathbf{F}}$$

$$\mathbf{E} = \frac{2}{N_T}\begin{bmatrix} 1/2 & 1/2 & \cdots & 1/2 \\ \cos\tau_0 & \cos\tau_1 & \cdots & \cos\tau_{2N_H} \\ \sin\tau_0 & \sin\tau_1 & \cdots & \sin\tau_{2N_H} \\ \cos 2\tau_0 & \cos 2\tau_1 & \cdots & \cos 2\tau_{2N_H} \\ \sin 2\tau_0 & \sin 2\tau_1 & \cdots & \sin 2\tau_{2N_H} \\ \vdots & \vdots & & \vdots \\ \cos N_H\tau_0 & \cos N_H\tau_1 & \cdots & \cos N_H\tau_{2N_H} \\ \sin N_H\tau_0 & \sin N_H\tau_1 & \cdots & \sin N_H\tau_{2N_H} \end{bmatrix}_{N_T\times N_T}$$

- The time domain variables are represented at uniformly spaced intervals for one period of oscillation

$$\tilde{\mathbf{Q}} = \begin{bmatrix} x_1(t_0) & \cdots & x_{N_{dof}}(t_0) \\ \vdots & x_i(t_n) & \vdots \\ x_1(t_{2N_H}) & \cdots & x_{N_{dof}}(t_{2N_H}) \end{bmatrix}_{(N_T)\times(N_{dof})} \qquad t_n = \frac{2\pi n}{\omega N_T}$$

- HDHB system can be written in terms of a time-derivative operator **D**

$$\omega^2\mathbf{D}^2\tilde{\mathbf{Q}}\mathbf{M} + \omega\mathbf{D}\tilde{\mathbf{Q}}\mathbf{C} - \tilde{\mathbf{F}} = \mathbf{0} \qquad \mathbf{D} = \mathbf{E}^{-1}\mathbf{A}\mathbf{E}$$

- Solution can be obtained numerically using an iterative root-finding scheme; Newton-Raphson method or pseudo-time marching

Features of the HDHB approach

- Advantages
  - Solves for one period of steady-state response; computationally efficient
  - Solved for in the time-domain
  - Easy implementation into large-scale computational fluid and structural dynamics codes
- Drawbacks

  Possibility of aliasing
  - Can produce nonphysical solutions
  - Due to treatment of nonlinear terms
  - Developed dealiasing techniques
  - Involves filtering of the field variables

  Memory required > time-marching
  - Fully populated solution arrays; N_T x N_{dof}

Typical time-marching solution

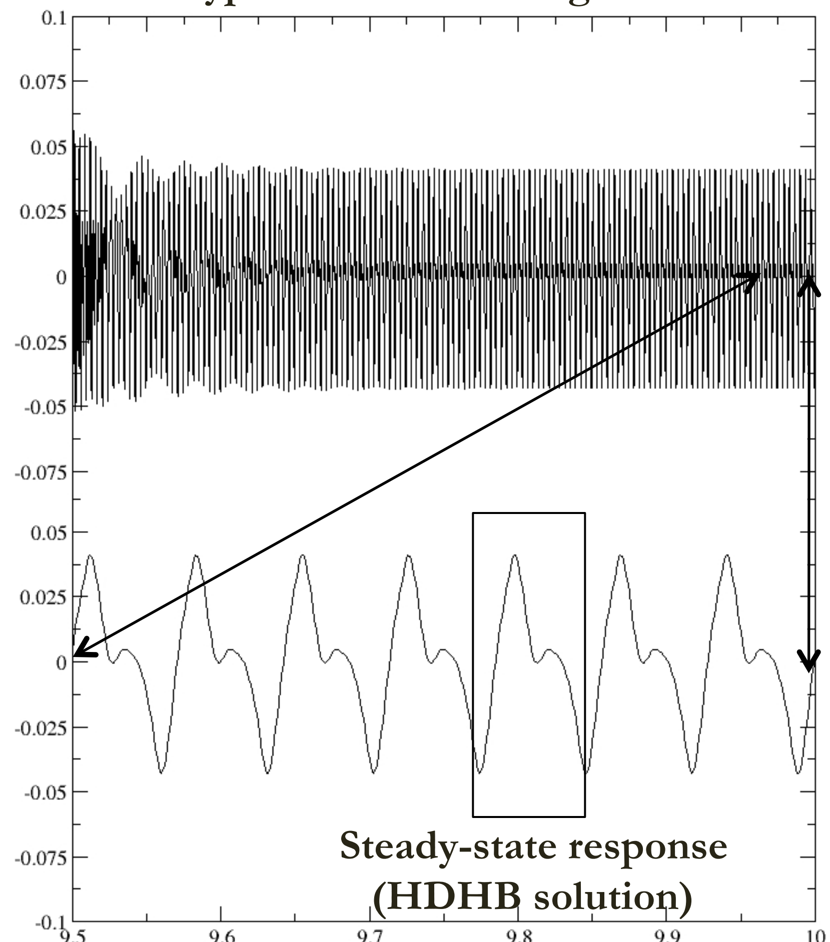

Steady-state response (HDHB solution)

Implementation into a FE solver

- Framework presented here has been successfully implemented into an in-house FE solver named ATFEM
- Begin with HDHB formulation of FE equations

$$\omega^2 \mathbf{D}^2 \tilde{\mathbf{Q}} \mathbf{M} + \omega \mathbf{D} \tilde{\mathbf{Q}} \mathbf{C} - \tilde{\mathbf{F}} = \mathbf{0}$$

- Solve the HDHB system using the Newton-Raphson (NR) method
  - The solution array ($\mathbf{Q}$) requires an initial guess; likely to be incorrect
  - The total residual ($\mathbf{R}_{\mathrm{TOT}}$) is the sum of partial residuals

$$\tilde{\mathbf{R}}_{\mathrm{TOT}} = \tilde{\mathbf{R}}_{\mathrm{DYN}} + \tilde{\mathbf{R}}_{\mathrm{DAMP}} + \tilde{\mathbf{R}}_{\mathrm{INT}} - \tilde{\mathbf{R}}_{\mathrm{EXT}} \qquad \tilde{\mathbf{R}}_{\mathrm{DYN}} = \omega^2 \mathbf{D}^2 \tilde{\mathbf{Q}} \mathbf{M} \qquad \tilde{\mathbf{R}}_{\mathrm{DAMP}} = \omega \mathbf{D} \tilde{\mathbf{Q}} \mathbf{C}$$

  - Incrementally adjust $\mathbf{Q}$ using the Jacobian matrix ($\mathbf{J}$) until $\mathbf{R}_{\mathrm{TOT}} = \mathbf{0}$

$$\Delta \tilde{\mathbf{Q}} = -\mathbf{J}^{-1} \tilde{\mathbf{R}}_{\mathrm{TOT}} \qquad \mathbf{J} = \frac{\partial \tilde{\mathbf{R}}_{\mathrm{TOT}}}{\partial \tilde{\mathbf{Q}}} = \frac{\partial \tilde{\mathbf{R}}_{\mathrm{DYN}}}{\partial \tilde{\mathbf{Q}}} + \frac{\partial \tilde{\mathbf{R}}_{\mathrm{DAMP}}}{\partial \tilde{\mathbf{Q}}} + \boxed{\frac{\partial \tilde{\mathbf{R}}_{\mathrm{INT}}}{\partial \tilde{\mathbf{Q}}} - \frac{\partial \tilde{\mathbf{R}}_{\mathrm{EXT}}}{\partial \tilde{\mathbf{Q}}}}$$

$$\frac{\partial \tilde{\mathbf{R}}_{\mathrm{DYN}}}{\partial \tilde{\mathbf{Q}}} = \omega^2 \mathbf{D}^2 \mathbf{M} \qquad \frac{\partial \tilde{\mathbf{R}}_{\mathrm{DAMP}}}{\partial \tilde{\mathbf{Q}}} = \omega \mathbf{D} \mathbf{C}$$

Readily available in any FE solver with implicit time-integration

- No major modifications to the FE data structure are required!

Plunging 1D string

- String membrane stretched between two rigid airfoils
- Geometrically nonlinear 1D string elements

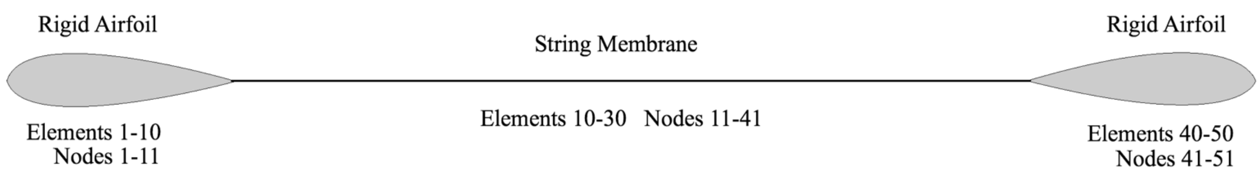

- Material properties:
  - Result in a first natural frequency of $f_1 = 14.2$ Hz

$E_{string} = 3\times10^5$ Pa	String modulus
$L_0 = 0.137$ m	String length
$A = 2.74\times10^{-4}$ m^2	Cross-sectional area
$\rho_0 = 0.274$ kg/m	Density per unit length
$T_0 = 4.11$ N	String pre-tension
$C = 0.05$	Viscous damping coefficient

- Flapping is implemented with time-periodic boundary conditions
  - Inertial loading is related to the flapping acceleration
  - Simulations are normalized using the inertial loading parameter F

$$w(X,t) = A\sin(\omega t) \qquad F = A\omega^2$$

Results for the plunging string

- Compare solutions obtained using the HDHB and HHTα time-marching methods
- Shown below: simulations for F = 100 (A = 0.05 and f = 7.1 Hz)
- HDHB approach renders steady state solutions 10^2-10^3 times faster than HHTα

Denotes $N_H = 2$

HHTα Solution

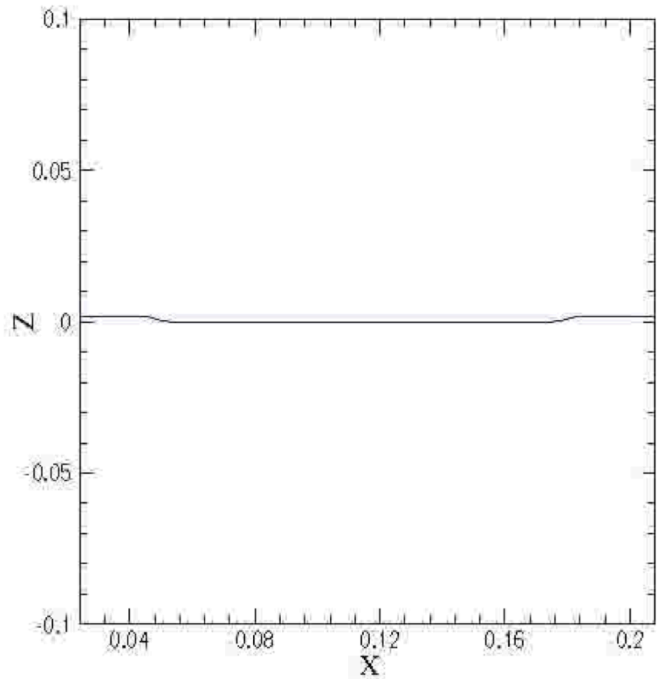

HDHB2 Solution

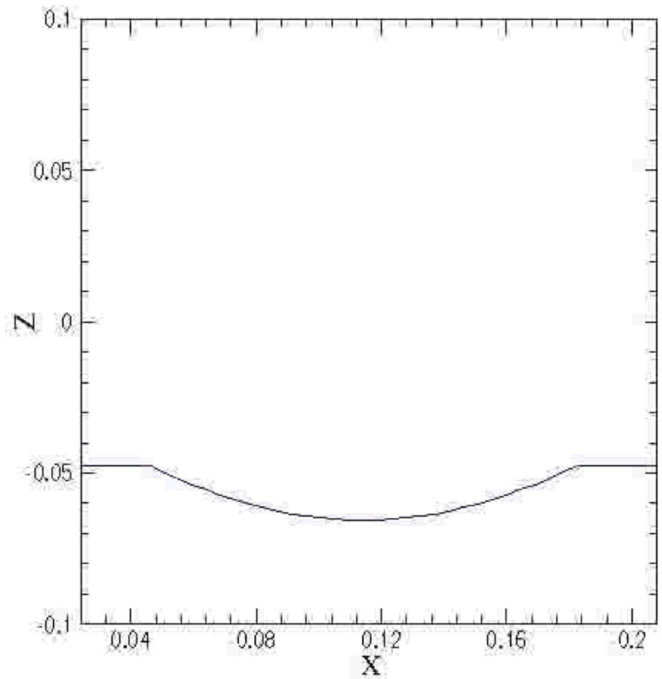

Frequency response curves

- Generated by incrementally advancing the frequency (ω) forward or backward
- Previous solution is used as the initial guess for the NR solver
- Frequency marching generates two solution branches: upper (+) and lower (-)
- Focus on the normalized midpoint Z-deflection ($w_{L/2}/L_0$)
- Favorable comparison between HDHB and HHTα solutions for $F = 0.1$ and 1
- Aliasing errors occur for $F = 10$ and 100; highly nonlinear
- Dealiasing techniques are not effective for this problem

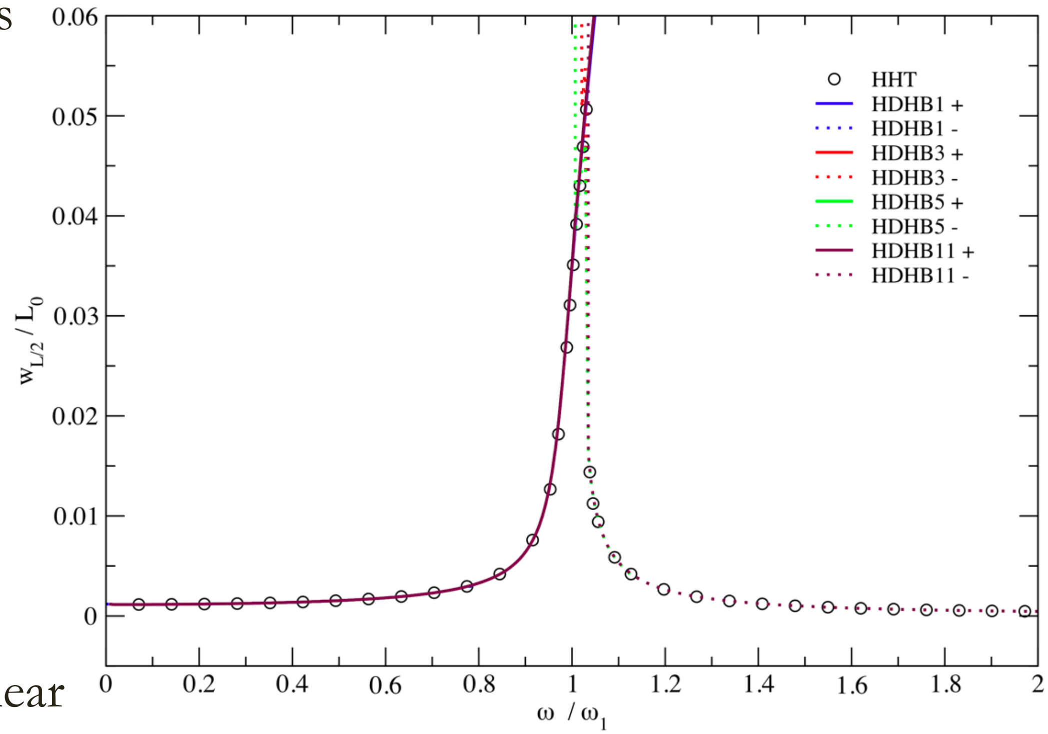

Frequency response curve for F = 1
Resonance peak at f = 14.6 Hz ($\omega/\omega_1 = 1.03$)

Flapping dragonfly wing

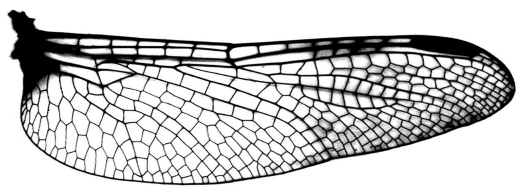

Dragonfly hindwing specimen

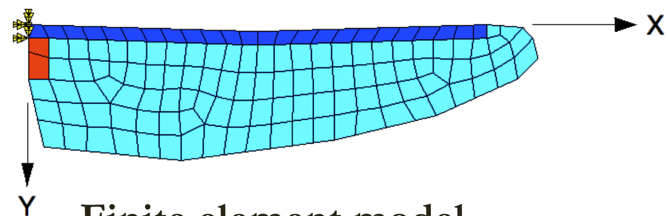

Finite element model

- Modeled using geometrically nonlinear von Karman plate elements
- Flapping motion—prescribed sinusoidal rotation about the root

$$\phi_0(t) = A\sin(2\pi f_0 t) \qquad A = 0.42045 \text{ rad} \qquad f_0 = 33.4 \text{ Hz}$$

- Material properties

Density	$\rho = 1200$ kg/m^3
Viscous damping	$C = 0.05$
Length	$L = 3$ cm
Poisson ratio	$\nu = 0.25$
1st natural frequency	$f_1 \approx 5f_0$

Strongest veins along leading edge (dark blue)
$E = 60$ Gpa $t = 0.135$ mm
Anal veins near root (red)
$E = 12$ GPa $t = 0.135$ mm
Wing membrane (light blue)
$E = 3.7$ GPa $t = 0.025$ mm

- HDHB solutions require amplitude marching (incremented by ΔA)
- HHTα solutions require marching from $t = 0$s to 2s with $\Delta t = 10^{-5}$s (τ~2 days)

HHTα solution

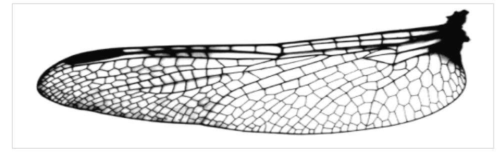

- Evolution of a transient response

Isometric view

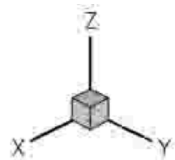

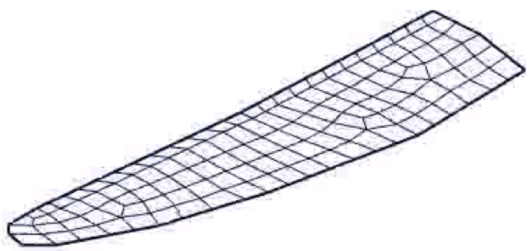

Rear view

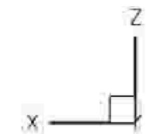

HDHB6 solution

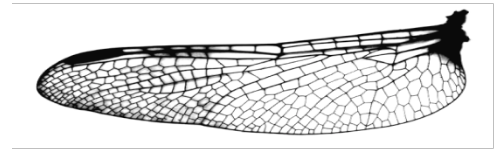

- Renders steady state response

Isometric view

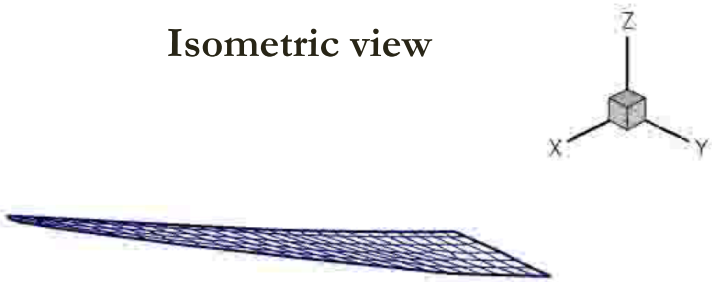

Rear view

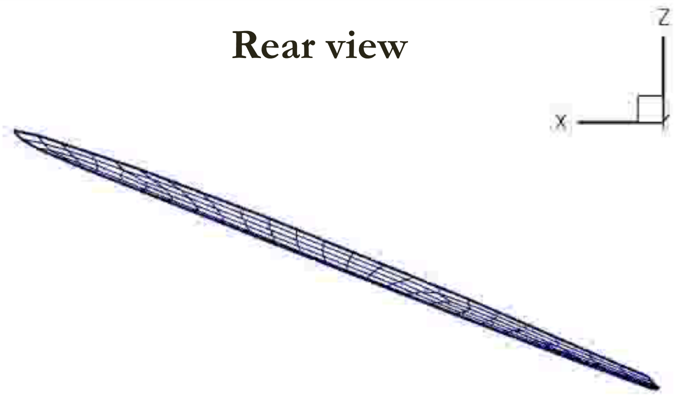

Computational economy

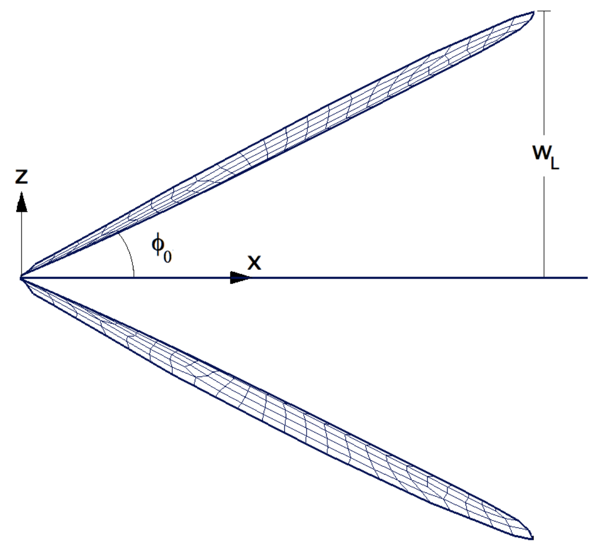

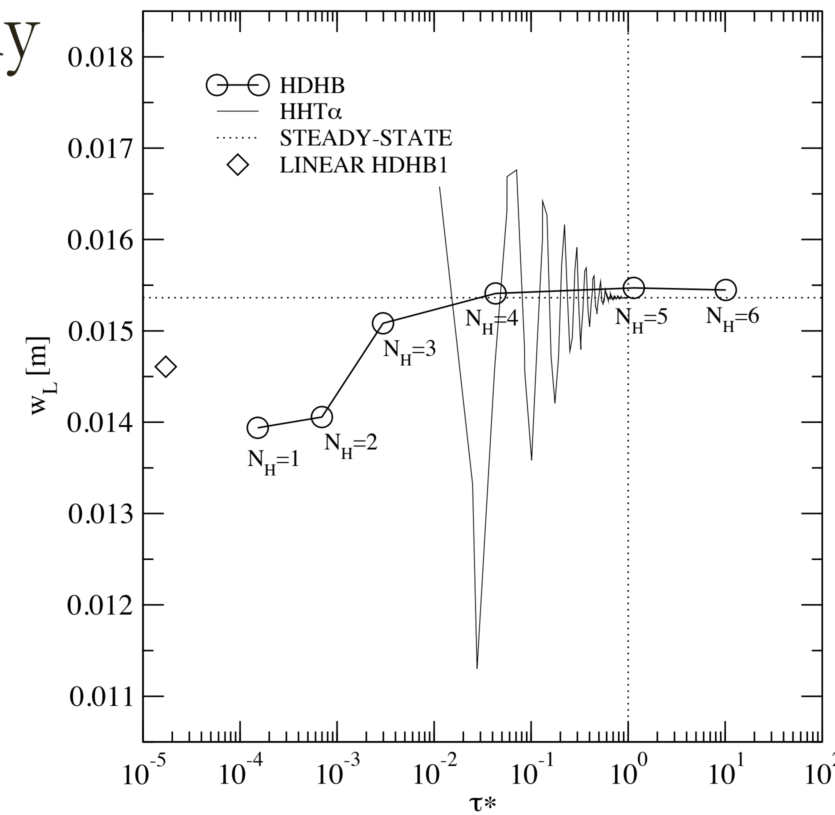

- Focus on peak displacement amplitudes (w_L)
- Increasing N_H requires more NR iterations and a smaller amplitude increment (ΔA)
- Normalized computation times (τ*) can be decreased by orders of magnitude

Method	ΔA (rad)	NR Iterations	τ^*
HHTα	–	–	1.000E+0
LIN HDHB	–	1	1.717E−5
HDHB1	0.1	29	1.522E−4
HDHB2	0.1	41	6.975E−4
HDHB3	0.1	105	2.979E−3
HDHB4	0.01	335	4.305E−2
HDHB5	0.0001	15,902	1.144E+0
HDHB6	0.00001	160,747	1.015E+1

Oscillating 3D continuum airfoil

- Modeled using geometrically nonlinear hexahedral elements with isoparametric interpolation (Q1)
- Approximately 10^4 spatial degrees of freedom
- Material properties

Elastic modulus	E = 70 GPa
Density	ρ = 2700 kg/m^3
Length	L = 3.41 m
Poisson ratio	ν = 0.33

- Prescribed sinusoidal boundary conditions at $z = L$

$$v(t) = A \sin(2\pi f_0 t)$$

A = 0.05 m
f_0 = 120 Hz

- HDHB solutions require amplitude marching with ΔA = 0.1m
- HHTα solutions require marching from t = 0s to 5s with Δt = 2 x10^{-5}s (τ~9 days)

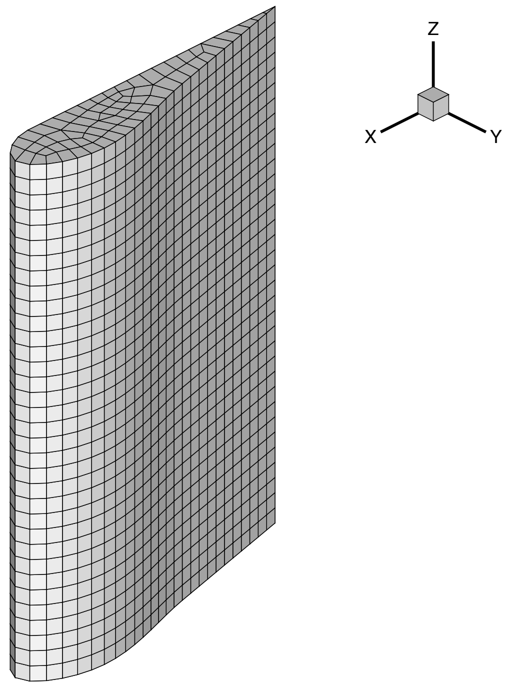

Finite element model

Solutions for 3D airfoil

- Focus on first principal stresses (σ_1) at a fixed location in space
- Compare maximum stress (σ_1^{max}) for each period of oscillation

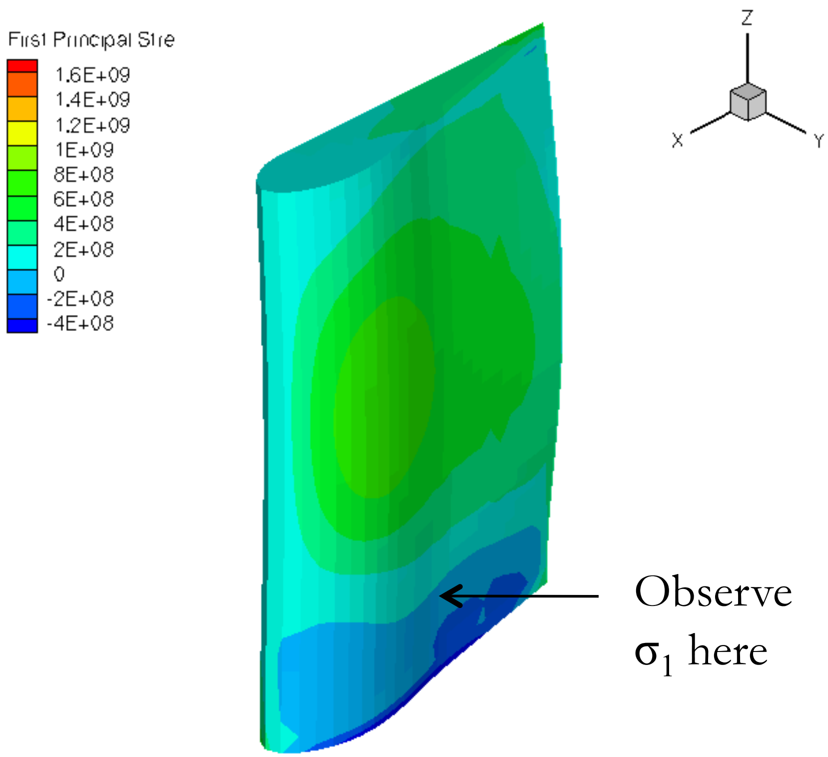

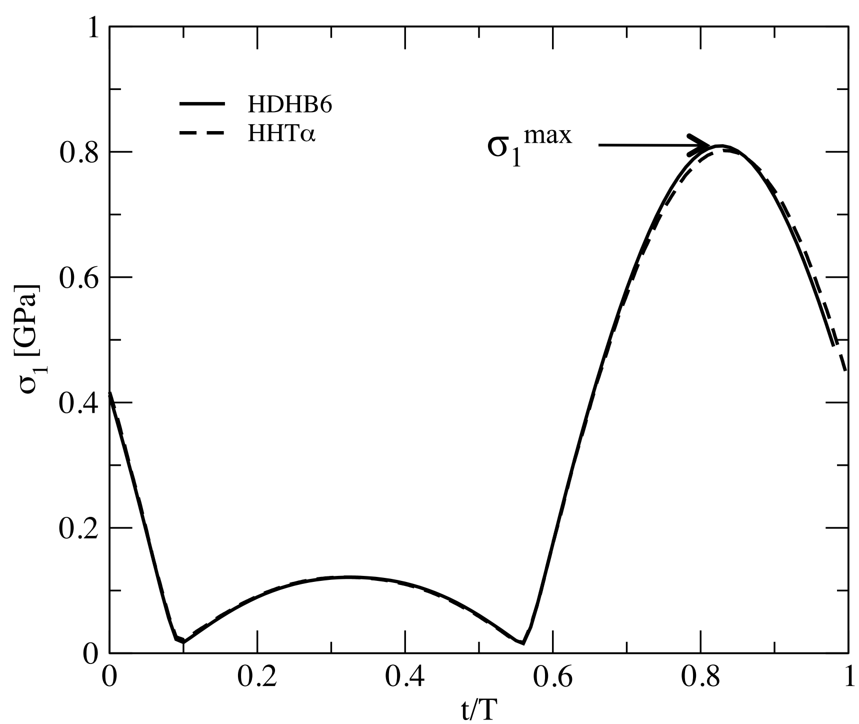

Computational economy

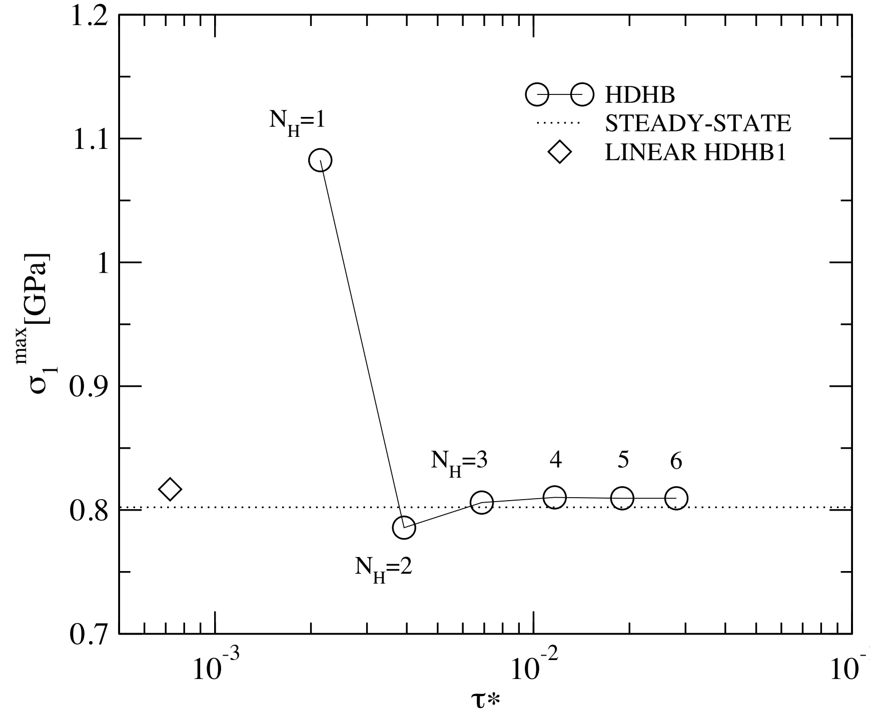

- Compare steady state values for maximum first principal stress (σ_1^{max})
- Normalized computation times (τ^*) indicate computational economy
- For this problem, choice of N_H does not affect # of NR iterations
- Required memory increases dramatically with N_H, necessitating the use of a supercomputer (OSCER)

➡ Memory can be a key limitation to HDHB approach

Method	NR iterations	Max memory (GB)	τ^*
HHTα	–	0.074	1.000E+0
LIN HDHB	1	0.512	7.228E–4
HDHB1	32	0.562	2.141E–3
HDHB2	30	1.604	3.922E–3
HDHB3	30	3.171	6.877E–3
HDHB4	30	5.374	1.165E–2
HDHB5	31	8.072	1.898E–2
HDHB6	31	11.216	2.809E–2

Conclusions

- Advantages of HDHB approach
  - Allows for rapid computation of steady state solutions for time-periodic problems
  - Can be orders of magnitude faster than time-marching
  - Easy implementation into computational fluid and structural dynamics codes
  - No major changes need to be made to the existing FE data structure
- Drawbacks
  - Aliasing may occur, especially for highly nonlinear problems; Dealiasing techniques have been developed
  - More memory is required compared to time-marching schemes; May become an issue for large-scale problems
- Future research
  - Investigate more efficient ways to solve the HDHB system of equations (other than the standard NR method presented here)
  - Coupling HDHB solvers for multiphysics problems, i.e., aeroelastic problems

References

Presentation adapted from

A. LaBryer and P. J. Attar. A Harmonic Balance Approach for Large-Scale Problems in Nonlinear Structural Dynamics. Journal of Computers and Structures, 88 (17-18) (2010) 1002-1017.

[1] Kryloff N, Bogoliuboff N. Introduction to nonlinear mechanics. Princeton, NJ: Princeton University Press; 1947.
[2] Aprille TJ, Trick TN. Steady-state analysis of nonlinear circuits with periodic inputs. Proc IEEE 1972;60(1):108–14.
[3] Nastov O. Spectral methods for circuit analysis. PhD thesis, Massachusetts Institute of Technology; 1999.
[4] Beran P, Petit C. A direct method for quantifying limit cycle oscillation response characteristics in the presence of uncertainties. AIAA paper 2004–1695.
[5] Kim Y, Noah S, Choi Y. Periodic response of multi-disk rotors with bearing clearances. J Sound Vibr 1991;144(3):381–95.
[6] McMullen M, Jameson A, Alonso J. Acceleration of convergence to a periodic steady state in turbomachinery flows. AIAA paper 2001–0152.
[7] McMullen M. The application of nonlinear frequency domain methods to the Euler and Navier–Stokes equations. PhD thesis, Stanford University; 2001.
[8] Gopinath AK, Beran PS, Jameson A. Comparative analysis of computational methods for limit-cycle oscillations. AIAA paper 2006–2076.
[9] Dimitriadis G. Continuation of higher-order harmonic balance solutions for nonlinear aeroelastic systems. J Aircraft 2008;45(2):523–37.
[10] Hall KC, Thomas JP, Clark WS. Computation of unsteady nonlinear flows in cascades using a harmonic balance technique. AIAA J 2002;40(5):879–86.
[11] Thomas JP, Dowell JP, Hall KC. Nonlinear inviscid aerodynamic effects on transonic divergence, flutter, and limit cycle oscillations. AIAA J 2002;40(4):638–46.
[12] Liu L, Thomas JP, Dowell EH, Attar P. A comparison of classical and high dimensional harmonic balance approaches for a duffing oscillator. J Comput Phys 2006;215:298–320.
[13] LaBryer A, Attar PJ. High dimensional harmonic balance dealiasing techniques for a duffing oscillator. J Sound Vibr 2009;324:1016–38.
[14] Cheney W, Kincaid D. Numerical mathematics and computing. Belmont, CA: Brooks/Cole; 2004.
[15] Maple RC, King PI, Orkwis PD, Wolff JM. Adaptive harmonic balance method for nonlinear time-periodic flows. J Comput Phys 2004;193:620–41.
[16] Tannehill JC, Anderson DA, Pletcher RH. Computational fluid mechanics and heat transfer. second ed. Philadelphia, PA: Taylor and Francis; 1997.
[17] Hamming RW. Numerical methods for scientists and engineers. New York: McGraw-Hill; 1973.
[18] Boyd JP. Chebyshev and Fourier spectral methods. Berlin: Springer-Verlag; 1989.
[19] Canuto C, Haussaini MY, Quarteroni A, Zang TA. Spectral methods in fluid dynamics. Berlin: Springer-Verlag; 1987.
[20] Orszag SA. On the elimination of aliasing in finite difference schemes by filtering high-wavenumber components. J Atmos Sci 1971;28:1074.
[21] Hou TY, Li R. Computing nearly singular solutions using pseudo-spectral methods. J Comput Phys 2006;226:379–97.
[22] Lele SK. Compact finite difference schemes with spectral-like resolution. J Comput Phys 1992;103:16–42.
[23] Belytschko T, Liu WK, Moran B. Nonlinear finite elements for continua and structures. John Wiley and Sons; 2000.
[24] Weis-Fogh T. Quick estimates of flight fitness in hovering animals including novel mechanisms for lift production. J Exp Biol 1973;59:169–230.
[25] Rayner J. Thrust and drag in flying birds: applications to birdlike micro air vehicles. Fixed and flapping wing aerodynamics for micro air vehicle applications, vol. 195. Reston, VA: AIAA; 2001. p. 217–30.
[26] Lee JS. Numerical study on flapping-airfoil design and unsteady mechanism of two-dimensional insect wing. PhD thesis, Seoul National University; 2006.
[27] Isogai K, Shinmoto Y, Watanabe Y. Effects of dynamic stall on propulsive efficiency and thrust of flapping airfoil. AIAA J 1999;37(10):1145–51.
[28] Hall K, Hall S. A rational engineering analysis of the efficiency of flapping flight. Fixed and flapping wing aerodynamics for micro air vehicle applications, vol. 195. Reston, VA: AIAA; 2001. p. 217–30.
[29] Heathcote S, Wang Z, Gursul I. Effect of spanwise flexibility on flapping wing propulsion. J Fluid Struct 2008;24:183–99.
[30] Heathcote S, Gursul I. Flexible flapping airfoil propulsion. AIAA J 2007;45(5):1066–79.
[31] Lian Y, Shyy W, Viieru D, Zhang B. Membrane wing aerodynamics for micro air vehicles. Prog Aerospace Sci 2003;39:425–65.
[32] Shyy W, Ifju P, Viieru D. Membrane wing-based micro air vehicles. Appl Mech Rev 2005;58:283–301.
[33] Gordnier R, Visbal M. High fidelity computational simulation of a membrane wing airfoil (Invited). AIAA paper 2008-0614.
[34] O'Reilly RO, Holmes PJ. Non-linear, non-planar and non-periodic vibrations of a string. J Sound Vibr 1992;153(3):413–35.
[35] Molteno TC, Tufillaro NB. An experimental investigation into the dynamics of a string. Am J Phys 2004;72(9):413–35.

References

[36] Rubin MR, Gottlieb O. Numerical solutions of forced vibration and whirling of a non-linear string using the theory of a Cosserat point. J Sound Vibr 1996;197(1):85–101.

[37] Attar PJ, Gordnier R. High fidelity computational aeroelastic analysis of a plunging membrane airfoil. AIAA paper 2009–2472.

[38] LaBryer A, Attar PJ. Modeling the nonlinear structural dynamics of a plunging membrane airfoil using a high dimensional harmonic balance approach. AIAA paper 2009–2474.

[39] Rojratsirikul P, Wang Z, Gursul I. Unsteady aerodynamics of membrane airfoils. AIAA paper 2008–0613.

[40] Ferreira JV, Serpa AL. Application of the arc-length method in nonlinear frequency response. J Sound Vibr 2005;284(1):133–49.

[41] Thomas ALR, Taylor GK, Srgley RB, Nudds RL, Bomphrey RJ. Dragonfly flight: free-flight and tethered flow visualizations reveal a diverse array of unsteady lift-generating mechanisms, controlled primarily via angle of attack. J Exp Biol 2004;207:4299–323.

[42] Attar PJ. Some results for approximate strain and rotation tensor formulations in geometrically non-linear Reissner–Mindlin plate theory. Int J Non-Linear Mech 2008;43(2):81–99.

[43] Bao L, Hu J, Yu YL, Cheng P, Xu BQ, Tong BG. Viscoelastic constitutive model related to deformation of insect wing under loading in flapping motion. J Appl Math Mech 2006;26(6):741–8.

[44] Crisfield MA. Nonlinear finite element analysis of solids and structures, vol. 1. John Wiley and Sons; 1991.

[45] Dowell EH. Aeroelasticity of plates and shells. Leyden, The Netherlands: Noordhoff International Publishing; 1975.

[46] Cook RD, Malkus DS, Plesha ME, Witt RJ. Concepts and applications of finite element analysis. fourth ed. John Wiley and Sons; 2002.

[47] Adelfinger U, Ramm E. EAS-elements for two-dimensional, three-dimensional, plate and shell structures and their equivalence to HR-elements. Int J Numer Methods Eng 1993;36:1311–37.